June 18, 2015

Ms. # CELL-METABOLISM-D-14-00916R2

SUPPLEMENTARY FIGURES

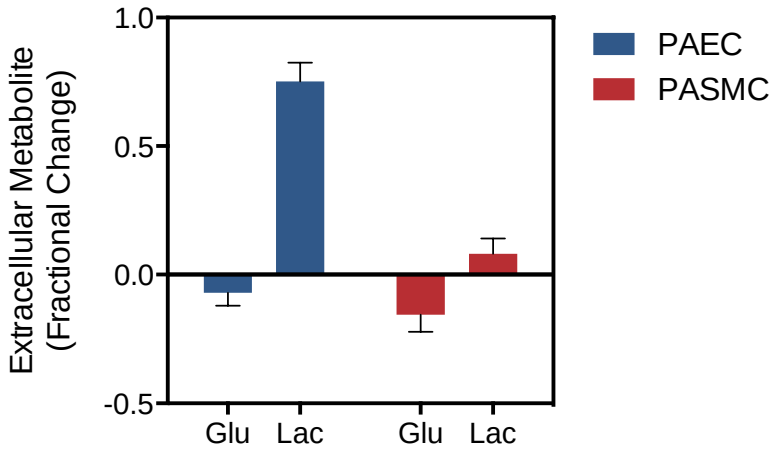

Figure S1. Hypoxia-mediated Metabolic Changes in Pulmonary Vascular Cells, related to Figure 1.

Fractional change in extracellular glucose and lactate in hypoxia-treated cells compared to 21% oxygen controls. PAEC, human pulmonary artery endothelial cells; PASMC, human pulmonary artery smooth muscle cells. Data are mean ± SEM.

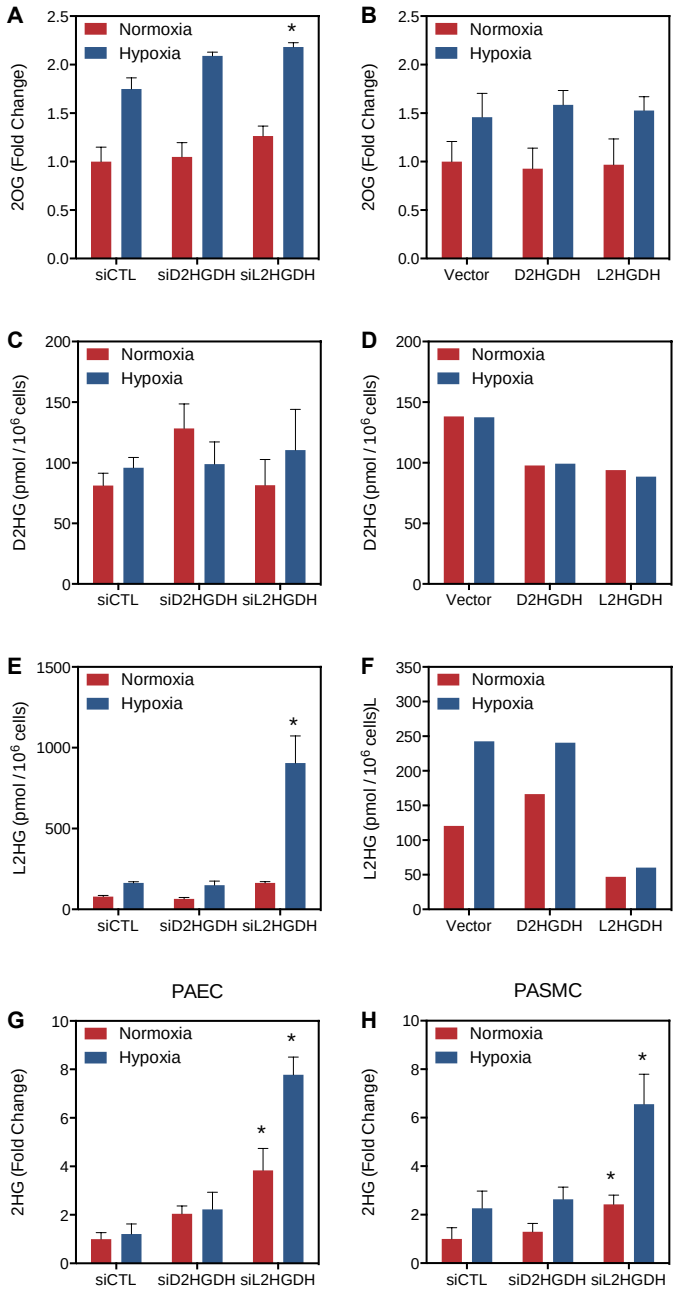

Figure S2. Hypoxia Preferentially Increases the L Enantiomer of 2HG, related to Figure 2. (A) 2OG in LF treated with siRNA targeted to D2HGDH or L2HGDH mRNA. (B) 2OG in LF expressing D2HGDH or L2HGDH compared with vector control. (C and D) D2HG levels measured in LF treated with 2HGDH knockdown (C) or overexpression (D) (N = 1). (E and F) L2HG levels measured in LF treated with 2HGDH knockdown (E) or overexpression (F) (N = 1). (G) 2HG in PAEC treated with siD2HGDH or siL2HGDH. (H) 2HG in PASMC treated with siD2HGDH or siL2HGDH. Data are mean ± SEM.

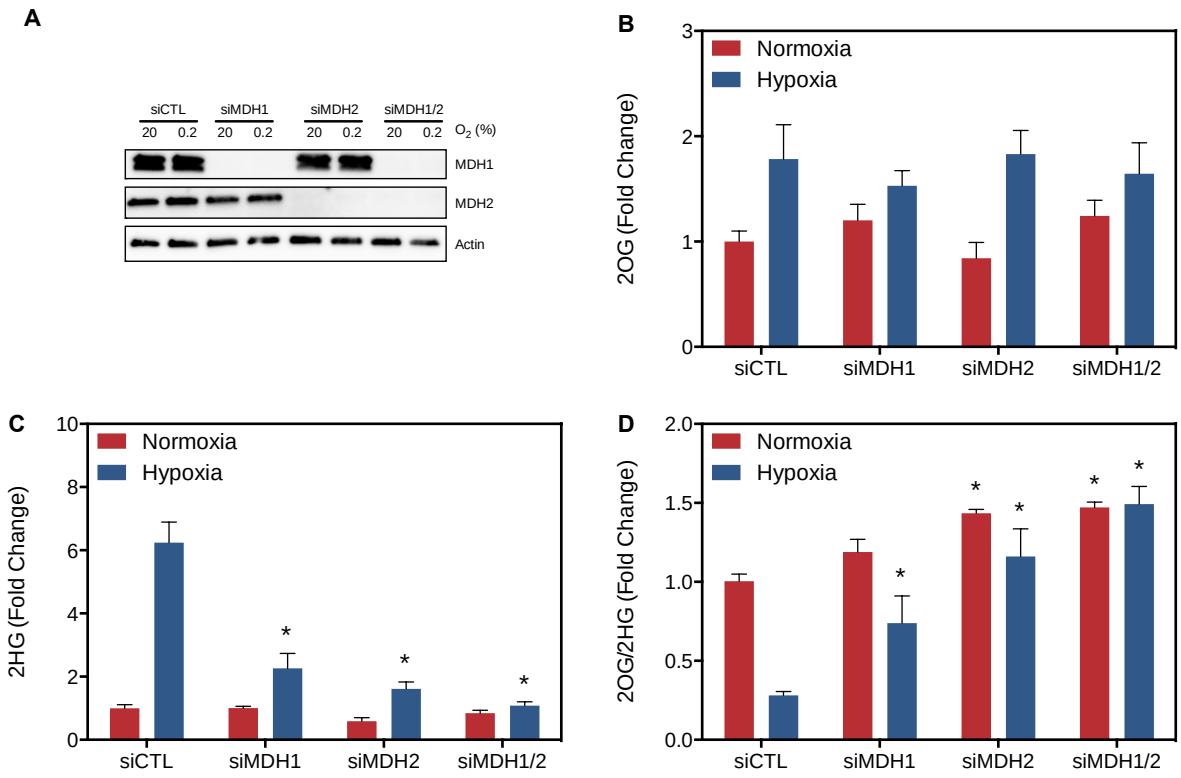

Figure S3. Consequences of malate dehydrogenase silencing in HEK cells, related to Figure 3. (A) Immunoblot of malate dehydrogenases 1 and 2 in HEK cell lysates. (B-D) Levels of 2HG (B), 2OG (C), and their ratio (D) in HEK cells exposed to hypoxia. Data are mean ± SEM.

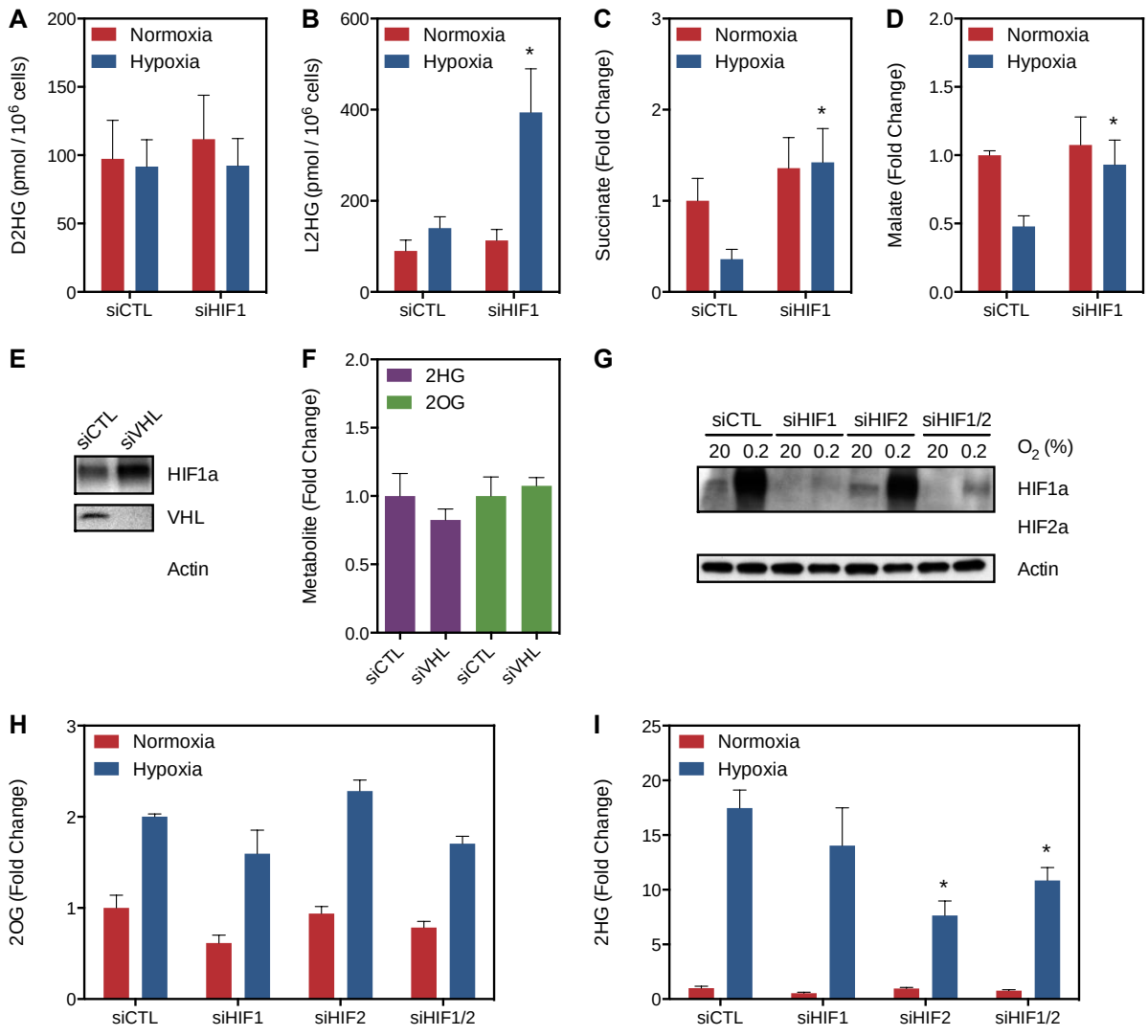

Figure S4. Role of HIF in 2HG Metabolism, related to Figure 4. (A and B) Direct analysis of 2HG enantiomers demonstrates that siHIF1 potentiates the hypoxia-mediated accumulation of L2HG in LF. (C and D) Succinate and malate determined in LF treated with siHIF1 compared to siCTL. (E-F) VHL suppression in HEK cells does not increase 2HG and 2OG metabolite levels in hypoxia. (G-I) 2HG accumulation in HEK cells is more sensitive to HIF2, rather than HIF1, silencing. Data are mean ± SEM.

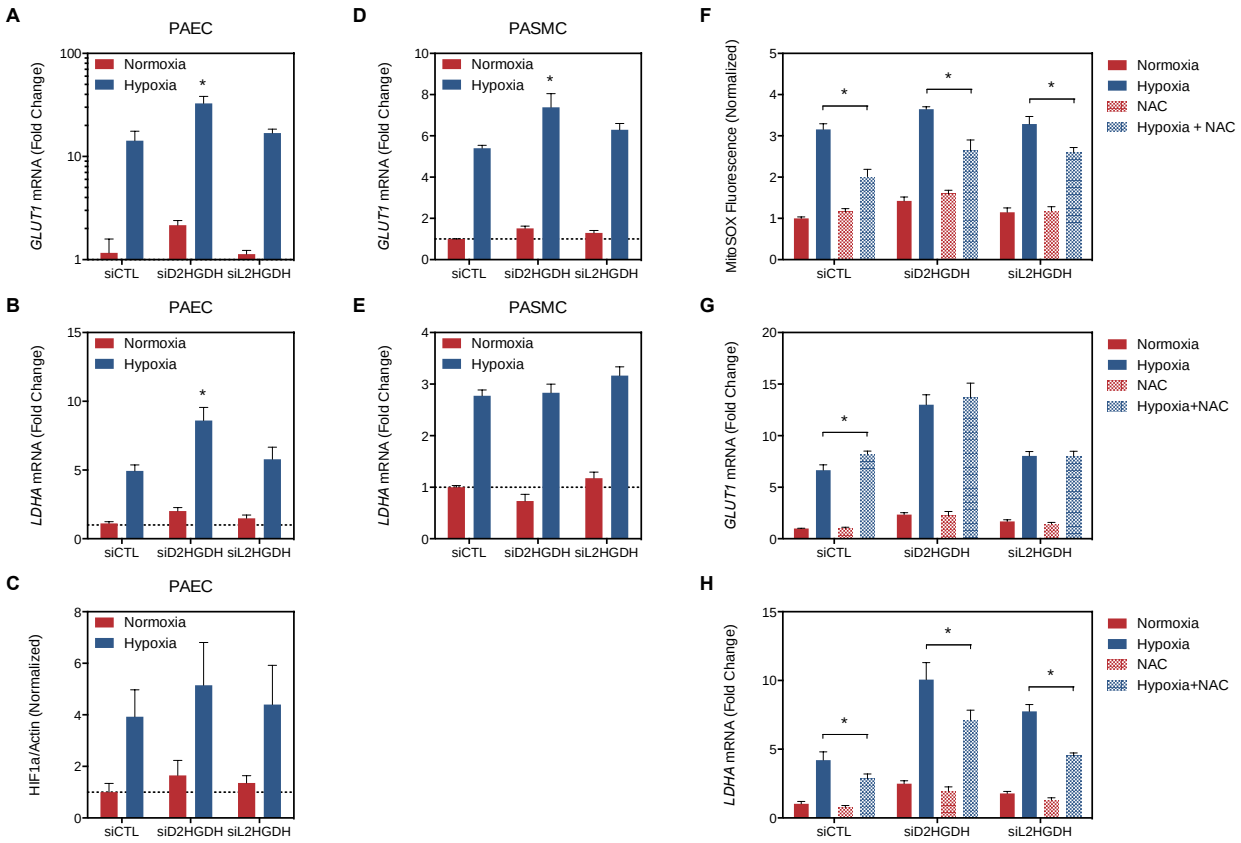

Figure S5. D2HGDH and L2HGDH Knockdown Activate HIF Target Gene Expression, related to Figure 5. (A-E) Similar to LF, 2HGDH knockdown in PAEC and PASMC results in increases in *GLUT1* and *LDHA* mRNA, and HIF1 protein expression in PAEC (C), suggesting activation of a HIF-dependent transcriptional program in these cells. Notably, *LDHA* was not induced in PASMC. (F-G) LF treatment with N-acetylcysteine for 24 h reduced hypoxia-stimulated superoxide production assessed by MitoSOX staining and decreased *LDHA* induction (H), although had a minimal impact on *GLUT1* mRNA levels (G). Data are mean ± SEM.

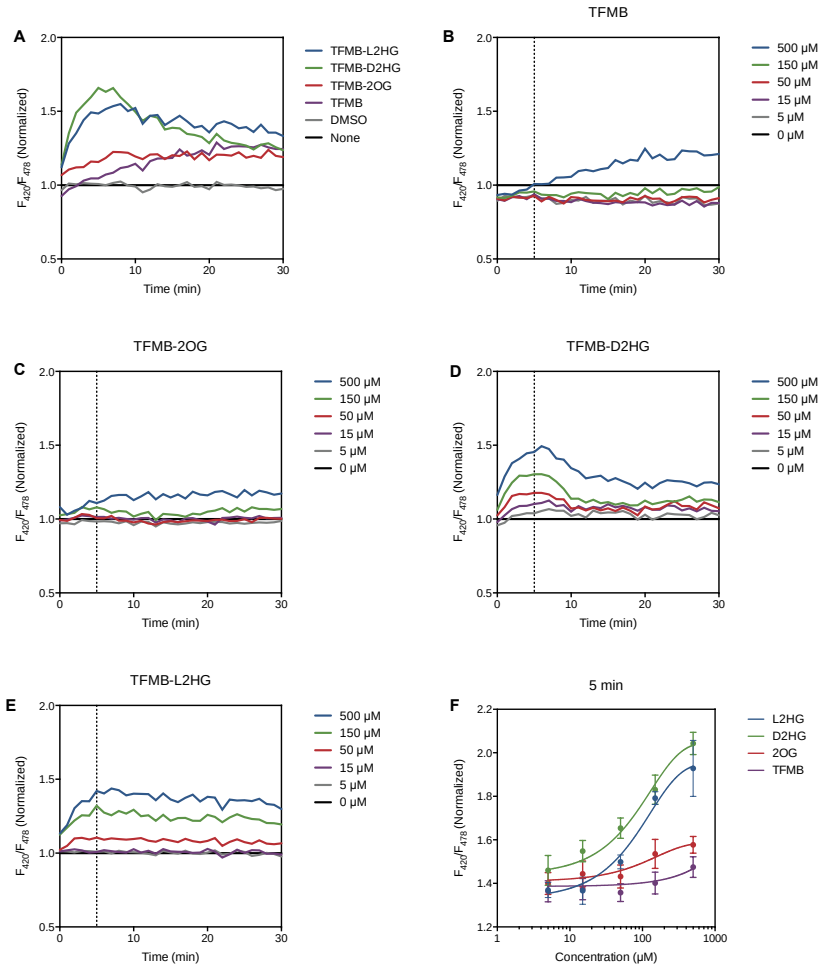

Figure S6. Cell-permeable analogues of 2HG increase cytoplasmic NADH/NAD$^+$, related to Figure 6. HEK cells transfected with the SoNar reporter were transfected with 500 μM cell-permeable analogue, DMSO vehicle, or TFMB alcohol (A). These fluorescence increases were dose-dependent for TFMB-D2HG and TFMB-L2HG (B-F). Data are mean ± SD of eight wells of a single experiment.

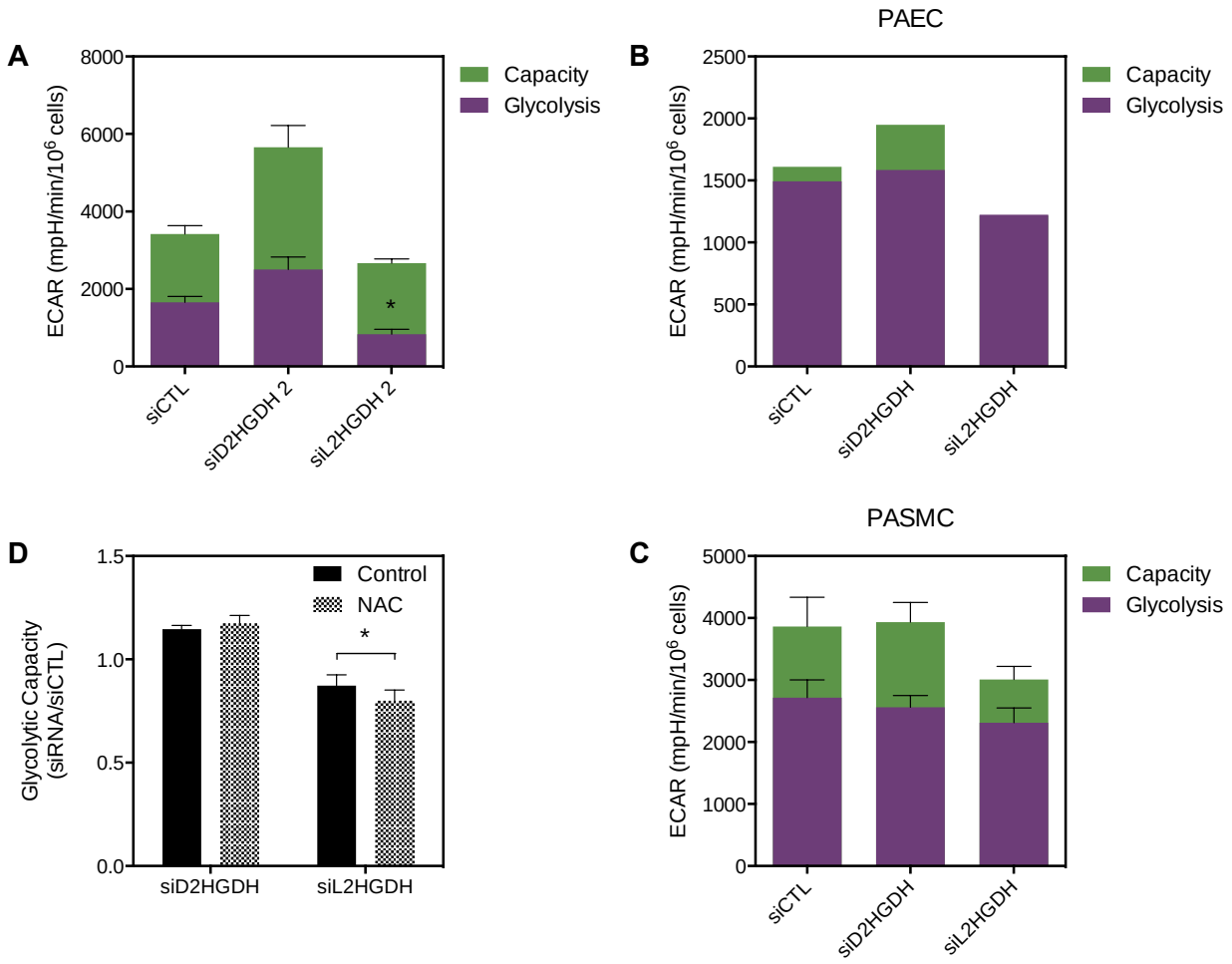

Figure S7. D2HGDH and L2HGDH Silencing Affects Glycolysis, related to Figure 7. (A) Different siRNA sequences targeting *D2HGDH* and *L2HGDH* have a similar effect on ECAR. (B and C) Silencing 2HGDH enzymes in PAEC (B) and PASMC (C) results in a similar phenotype as LF; however, PASMC do not demonstrate an increase in ECAR in siD2HGDH-treated cells (C). (D) NAC treatment did not reduce siD2HGDH-mediated activation of ECAR, but potentiated the siL2HGDH-mediated reduction of ECAR.

SUPPLEMENTAL TABLES

The spreadsheets contain the results of the metabolomics analysis in PAEC ("EC") and PASMC ("SMC") performed using Metaboanalyst according to the methods described in Supplementary Experimental Procedures below. The "Metabolites" spreadsheets list the metabolites significantly altered by hypoxia. Metabolites increased by hypoxia are highlighted in blue while metabolites decreased by hypoxia are highlighted in red. The "MSEA" spreadsheets list the results of metabolite set enrichment analysis for those pathways with a false discovery rate (FDR) q-value less than 0.05. "Total" refers to the number of metabolites included in that pathway while "Hits" refers to the number of metabolites identified as differentially regulated that are a component of that pathway. The "PATHWAY" spreadsheets are similarly reported and now include an "Impact" score that accounts for the effect of a given metabolic perturbation on the pathway based on its connectedness to other members of the pathway.

SUPPLEMENTAL TABLE LEGENDS

Table S1. Metabolites Differentially Regulated by Hypoxia, Related to Figure 1. Fold changes shown are hypoxia/normoxia levels. Those metabolites shaded blue are increased by hypoxia while those shaded red are decreased by hypoxia.

Table S2. Metabolite Set Enrichment Analysis, Related to Figure 1. Metabolite sets that were significantly affected by hypoxia treatment based on a quantitative enrichment analysis. Sets with a false discovery rate q-value less than 0.05 are listed for both PAEC and PASMC. "Total" refers to the number of metabolites in the set while "Hits" refers to the number of differentially regulated metabolites. The reference metabolome is based on the list of metabolites submitted for analysis.

Table S3. KEGG Pathway Network Analysis, Related to Figure 1. Similar to Table S2, this table lists KEGG Pathways that were significantly affected by hypoxia treatment based on an enrichment analysis. An "Impact" score (0-1) is calculated based on the relative importance of affected metabolites (*i.e.*, nodes) relative to the overall pathway structure.

SUPPLEMENTAL EXPERIMENTAL PROCEDURES

Reagents. Enantiomerically pure D2HG and L2HG and all other chemicals were purchased from Sigma unless otherwise noted. Cell-permeable trifluoromethylbenzyl (TFMB) esters of 2OG, D2HG, and L2HG were synthesized by WuXi AppTec (Losman et al., 2013; MacKenzie et al., 2007).

Metabolomic Screen. Cells were extracted with 80% aqueous methanol pre-cooled to -80 °C. Cell extracts were analyzed using targeted LC-MS methods as previously published (Jain et al., 2012). Cells were washed with one volume of ice-cold PBS and placed on dry ice. Metabolism was quenched with the immediate addition of 80% methanol in water pre-cooled to -80 °C. Cells were collected by scraping, vortexed, and centrifuged. The clarified supernatant was stored at -80 °C prior to analysis by LC-MS. Profiles of endogenous, water-soluble metabolites were obtained using targeted LC-MS methods operating in positive and negative ionization modes. Both methods were developed using reference standards of each metabolite to determine chromatographic retention times and MS multiple reaction monitoring transitions, declustering potentials, and collision energies. Negative ionization mode data were acquired using an ACQUITY UPLC (Waters) coupled to a 5500 QTRAP triple quadrupole mass spectrometer (AB SCIEX). Cell extracts (10 µL) were injected onto a 150- × 2.0-mm Luna NH2 column (Phenomenex) that was eluted at a flow rate of 400 µL/min with initial conditions of 10% mobile phase A (20 mM ammonium acetate and 20 mM ammonium hydroxide in water) and 90% mobile phase B (10 mM ammonium hydroxide in 75:25 vol/vol acetonitrile/methanol) followed by a 10-min linear gradient to 100% mobile phase A. The ion spray voltage was −4.5 kV and the source temperature was 500 °C. Positive ionization mode data were acquired using a 4000 QTRAP triple quadrupole mass spectrometer (AB SCIEX) coupled to an 1100 Series pump (Agilent) and an HTS PAL autosampler (Leap Technologies). The samples (10 µL) were injected onto a 150- × 2.1-mm Atlantis HILIC column (Waters). The column was eluted isocratically at a flow rate of 250 µL/min with 5% mobile phase A (10 mM ammonium formate and 0.1% formic acid in water) for 1 min followed by a linear gradient to 40% mobile phase B (acetonitrile with 0.1% formic acid) over 10 min. The ion spray voltage was 4.5 kV and the source temperature was 450 °C. Data were analyzed using MultiQuant software (AB SCIEX).

Peak areas were normalized to protein content from duplicate plates of cells treated in parallel. Metabolomics data were analyzed using Metaboanalyst 2.0 (Xia et al., 2012; Xia et al., 2009). Metabolites with a single or constant value across samples were eliminated from analysis. Assuming that the remaining missing values represented metabolites below the detection limit, these were replaced with a small value (half of the minimum positive value in the data) as a placeholder. Peak areas were normalized to cellular protein content determined from plates treated in parallel, log transformed, and scaled. Pathway enrichment and topology analyses were performed. Results of this analysis are summarized in Supplemental Tables 1-3.

Targeted LC-MS. Metabolites were extracted in cold 80% methanol. Prior to scraping, samples were spiked with [$^{13}C_4$]-2OG at 5 µM final concentration (Cambridge Isotope Laboratories) as an internal standard (ISTD). Metabolites were separated in HILIC mode using a ZIC-HILIC (150 mm x 2.1 mm x 3.5 µm; Merck) stationary phase. Mobile phases were prepared from 10% 200 mM ammonium acetate, pH 3.7, in acetonitrile (A) or water (B). The HPLC method used an injection volume of 5 µL and a linear gradient from 0% to 80% B at a flow rate of 200 µL/min with a Surveyor HPLC system coupled by negative electrospray ionization to a Finnigan LTQ linear ion trap mass spectrometer (Thermo Scientific) operating in multiple reaction monitoring mode with MS parameters optimized using a 2HG standard solution. Monitored transitions were 147 → 129 (2HG, R_t 10.3 min), 145 →101 (2OG, R_t 10.1 min), 133 → 115 (malate, R_t 10.6 min), 115 →73 + 99 (succinate, R_t 4.7 min), and 149 → 105 (ISTD, R_t 10.1 min). Retention time windows were confirmed by the analysis of neat and matrix-spiked standards. Peak areas were quantified by Xcalibur Software (Thermo) and manually reviewed. Concentrations were determined by interpolating the peak area ratio of analyte to ISTD from a standard curve (0.1-10 µM neat standards). Concentrations were normalized to cell count determined by Z2 Coulter Counter (Beckman Coulter) from plates of cells treated in parallel.

Quantification of 2HG Enantiomers. Briefly, 200 µL cell extract was evaporated to dryness under vacuum at 65 °C in a SpeedVac evaporator (Thermo). The residue was resuspended in 50 µL freshly

prepared 50 mg/mL DATAN in 4:1 (by volume) acetonitrile:acetic acid and heated at 75 °C for 30 min. After cooling to room temperature, the samples were briefly centrifuged, and 50 µL 4:1 acetonitrile:acetic acid was added. Enantiomers were separated using a ZIC-HILIC stationary phase. The HPLC method used an injection volume of 5 µL and isocratic flow of 15% B for 13 min followed by a wash at 80% B and re-equilibration at 15% B at a flow rate of 150 µL/min. MS parameters were optimized using a DATAN-2HG standard solution.

RNA Interference. The following Silencer Select small interfering RNA reagents were used (Life Technologies): non-targeting control (4390846), *D2HGDH* (s58478 and s58479), *L2HGDH* (s36693 and s36692), *MDH1* (s8621), *MDH2* (s8622), *VHL* (s14789), *HIF1A* (s6539), and *EPAS1* (s4700). Cells were reverse-transfected with Lipofectamine RNAiMAX (Life Technologies) according to the manufacturer's protocol. Knockdown efficiency was determined by RT-qPCR 72 h following transfection and Western immunoblot. Dual knockdown experiments used the same total siRNA concentration as single knockdown experiments.

D2HGDH and L2HGDH Overexpression. Human cDNA ORF clones of D2HGDH (RC207367) and L2HGDH (RC217631) were purchased from Origene. These were subcloned into a lentiviral expression vector in frame with C-terminal HA tag (LV022, ABM). HEK cells were transfected with pLenti-D2HGDH, pLenti-L2HGDH, or pLenti-Vector using Lipofectamine 2000 according to the manufacturer's protocol (Life Technologies).

Analysis of mRNA Levels. Total RNA was isolated from cells with the RNeasy Mini Kit (Qiagen) using DNase I. cDNA was synthesized from 500 ng RNA with the Advantage RT for PCR kit (Clontech) using oligo-dT primers. RT-qPCR analysis was performed with an Applied Biosystems 7500 Fast Real Time PCR system with TaqMan Universal PCR Master Mix and the following pre-designed TaqMan gene expression assays (Life Technologies): *POLR2A* (Hs00172187_m1), *D2HGDH* (Hs00292260_m1), *L2HGDH* (Hs00227575_m1), *MDH1* (Hs00936497_g1), *MDH2* (Hs00938918_m1), *VHL* (Hs03046964_s1), *GLUT1* (*SLC2A1*, Hs00892681_m1), *HIF1A* (Hs00153153_m1), *EPAS1*

(Hs01026149_m1), and *LDHA* (Hs00855332_g1). Relative expression levels were calculated using the comparative cycle threshold method referenced to *POLR2A*.

Lentivirus Production and Transduction. Lentiviruses were produced by transfecting HEK293T cells with a lentiviral vector and packaging plasmids pMD2.G and psPAX2 (Addgene plasmids 12259 and 12260, D. Trono) using Lipofectamine 2000 (Life Technologies) according to the manufacturer's protocol. Virus-containing supernatants were collected at 24 and 28 h following transfection, filtered through a 0.45 μm PVDF membrane, and used immediately or stored at -80 °C. Cells were transduced for 24 h with medium containing viral particles and 8 μg/mL polybrene.

Western Immunoblotting. Cells were washed twice with one volume PBS and lysed in Cell Lysis Buffer (Cell Signaling Technology) containing Protease Inhibitor Cocktail III (Calbiochem) by sonication. Cell debris was pelleted by centrifugation at 21,100 *g* at 4 °C for 15 min. Lysates were normalized for protein concentration and subjected to SDS-PAGE, transferred to PVDF membranes, blotted, developed, and analyzed as described previously (Kao et al., 2013). Primary antibodies used were: Actin (A2066, Sigma), L2HGDH (15707-1-AP, ProteinTech), D2HGDH (13895-1-AP, ProteinTech), MDH1 (NBP1-89515, Novus Biologicals), MDH2 (ab96193, Abcam), VHL (2738S, Cell Signaling), HIF1α (NB100-134, Novus Biologicals), and HIF2α (NB100-122). HRP-conjugated secondary antibodies were: rabbit (7074, Cell Signaling Technology) and mouse (A4416, Sigma).

NADH/NAD$^+$ Enzymatic Assay. Cellular NAD$^+$ and NADH were measured using an adaptation of a previously published enzymatic fluorimetric cycling assay based on the reduction of NAD$^+$ to NADH by alcohol dehydrogenase (ADH) and subsequent electron transfer to generate the fluorescent molecule resorufin (Umemura and Kimura, 2005; Zhu and Rand, 2012). Briefly, cells were washed twice with one volume PBS. Pyridine nucleotides were extracted on ice with buffer containing 50% by volume PBS and 50% lysis buffer (100 mM sodium carbonate, 20 mM sodium bicarbonate, 10 mM nicotinamide, 0.05% by volume Triton-X-100, 1% by mass dodecyltrimethylammonium bromide) and collected by scraping. Extracts were divided equally and 0.5 volume of 0.4 N HCl was added to one sample. Both extracts were

heated at 65 °C for 15 min to degrade selectively either the oxidized (buffer) or reduced (HCl) nucleotides. The reaction was cooled on ice and quenched by adding 0.5 M Tris-OH to the acid-treated samples or 0.2 N HCl plus 0.25 M Tris-OH to the buffer samples. Samples were then diluted in reaction buffer (50 mM EDTA and 10 mM Tris, pH 7.06). Cell debris was pelleted by centrifugation, and 50 µL was incubated for 2 h with 100 µL reaction buffer containing 0.6 M EtOH, 0.5 mM phenazine methosulfate, 0.05 mM resazurin, and 0.1 mg/mL ADH. Fluorescence intensities were measured with a Spectramax Gemini XPS (Molecular Devices) with excitation 540 nm, emission 588 nm, and 550 nm excitation cut-off filter. Sample intensities were compared to a standard curve generated from known concentrations of NADH. The ratio of fluorescence in buffer-extracted to acid-extracted samples corresponds to the NADH/NAD^+ ratio. Absolute NADH and NAD^+ were normalized to cell count from cells treated in parallel.

Intracellular NADH/NAD^+ Sensor. SoNar is a recently developed genetically encoded fluorescence sensor of NADH/NAD^+ constructed from the fusion of the *T. aquaticus* Rex NAD(H) binding domain to cyclically permuted YFP (cpYFP). This construct has different excitation wavelengths when bound to NADH (420 nm) and NAD^+ (485 nm) and demonstrates a linear response to a wide range of NADH/NAD^+ (0.001-1) (Zhao et al., 2015). The Sonar ORF was subcloned into the pLenti-III-HA vector (ABM) using the *NheI* and *XhoI* restriction sites for lentivirus production. SoNar-expressing cells were plated 48 h prior to measurement in 96-well plates. For siRNA experiments, cells were reverse transfected into 96-well plates 48 h prior to the experiment. Prior to the assay, the growth medium was removed and 100 µL warmed HEPES buffered saline solution was added. Subsequently, 100 µL of 1 mM test compound was added and the plate was read in a SpectraMax M3 fluorescence plate reader (Molecular Devices) using dual excitation wavelengths of 420 nm and 478 nm and an emission wavelength of 530 nm. The background fluorescence from wells containing 200 µL HBSS was subtracted at each excitation wavelength. Subsequently, the F_{420}/F_{478} ratio was calculated and normalized to the fluorescence of untreated cells.

REFERENCES

Kao, D.D., Oldebeken, S.R., Rai, A., Lubos, E., Leopold, J.A., Loscalzo, J., and Handy, D.E. (2013). Tumor necrosis factor-alpha-mediated suppression of dual-specificity phosphatase 4: crosstalk between NFkappaB and MAPK regulates endothelial cell survival. Mol Cell Biochem *382*, 153-162.

Losman, J.A., Looper, R.E., Koivunen, P., Lee, S., Schneider, R.K., McMahon, C., Cowley, G.S., Root, D.E., Ebert, B.L., and Kaelin, W.G., Jr. (2013). (R)-2-hydroxyglutarate is sufficient to promote leukemogenesis and its effects are reversible. Science *339*, 1621-1625.

MacKenzie, E.D., Selak, M.A., Tennant, D.A., Payne, L.J., Crosby, S., Frederiksen, C.M., Watson, D.G., and Gottlieb, E. (2007). Cell-permeating alpha-ketoglutarate derivatives alleviate pseudohypoxia in succinate dehydrogenase-deficient cells. Mol Cell Biol *27*, 3282-3289.

Umemura, K., and Kimura, H. (2005). Determination of oxidized and reduced nicotinamide adenine dinucleotide in cell monolayers using a single extraction procedure and a spectrophotometric assay. Anal Biochem *338*, 131-135.

Xia, J., Mandal, R., Sinelnikov, I.V., Broadhurst, D., and Wishart, D.S. (2012). MetaboAnalyst 2.0--a comprehensive server for metabolomic data analysis. Nucleic Acids Res *40*, W127-133.

Xia, J., Psychogios, N., Young, N., and Wishart, D.S. (2009). MetaboAnalyst: a web server for metabolomic data analysis and interpretation. Nucleic Acids Res *37*, W652-660.

Zhao, Y., Hu, Q., Cheng, F., Su, N., Wang, A., Zou, Y., Hu, H., Chen, X., Zhou, H.M., Huang, X., et al. (2015). SoNar, a Highly Responsive NAD(+)/NADH Sensor, Allows High-Throughput Metabolic Screening of Anti-tumor Agents. Cell Metab *21*, 777-789.

Zhu, C.T., and Rand, D.M. (2012). A hydrazine coupled cycling assay validates the decrease in redox ratio under starvation in Drosophila. PLoS One *7*, e47584.